

Cite this: *Chem. Sci.*, 2018, 9, 4808Received 28th March 2018  
Accepted 29th April 2018

DOI: 10.1039/c8sc01427b

rsc.li/chemical-science

## Silylation reactions on nanoporous gold via homolytic Si–H activation of silanes†

Hongbo Li,<sup>‡a</sup> Huifang Guo,<sup>‡a</sup> Zhiwen Li,<sup>b</sup> Cai Wu,<sup>a</sup> Jing Li,<sup>a</sup> Chunliang Zhao,<sup>a</sup> Shuangxi Guo,<sup>a</sup> Yi Ding,<sup>\*b</sup> Wei He<sup>id</sup> <sup>\*a</sup> and Yadong Li<sup>id</sup> <sup>c</sup>

Si–H bond activation is an important process implicated in many useful synthetic applications including silylation and transfer hydrogenation reactions. Herein we discovered homolytic activation of Si–H bonds on the surface of nanoporous gold (NPG), forming hydrogen radicals and [Au]–[Si] intermediates. By virtue of this new reactivity, we achieved highly selective mono and sequential alcoholysis of dihydrosilane. In addition, the amphiphilic nature of the [Au]–[Si] intermediate allows for a new bis-silylation reaction of cyclic ethers. The present work showcased that the surface reactivity of nanocatalysts may provide exciting opportunity for new reaction discovery.

## Introduction

Catalytic activation of Si–H bonds provides rapid construction of silicon-containing functional molecules or materials, a process collectively referred to as “silylation reactions”.<sup>1–4</sup> This also enables transfer hydrogenation reactions where the silanes serve as the hydrogen gas equivalent.<sup>5–8</sup> A plethora of homogeneous metal catalysts including Pd,<sup>9</sup> Ir,<sup>10–15</sup> Rh,<sup>16–18</sup> Ni,<sup>19,20</sup> Ru,<sup>21–24</sup> Co,<sup>25</sup> and Fe<sup>26–30</sup> salts had been discovered for these important processes. These homogeneous catalysts often activate silanes through oxidative addition or a  $\sigma$ -bond metathesis pathway, giving rise to metal hydride ([M]–H) intermediates.<sup>20,22,23,27</sup> The metal hydride is known to be highly reactive towards unsaturated bonds, thus posing considerable limitations on the substrate scope.<sup>22,23,29</sup>

There is an intriguing pattern in the past few decades that heterogeneous catalysts can display reactivity inaccessible by known homogeneous catalysts.<sup>31–33</sup> For example, Porco and co-workers reported an elegant silver nanoparticle catalysed Diels–Alder cycloaddition that was not catalysed by homogeneous Lewis acids.<sup>34</sup> Glorius and his colleagues discovered that Pd/C showed completely different regioselectivity in the arylation of benzothiophenes as compared to homogeneous Pd catalysts.<sup>35</sup> Recently, we reported a catalytic deoxygenation reaction of aromatic epoxides on the Cu surface, affording alkenes with high *cis* isomer selectivity.<sup>36</sup>

We thus became curious about Si–H activation on the surface of heterogeneous metal catalysts.<sup>37–39</sup> Importantly, the pioneering studies of Yamamoto,<sup>40</sup> Jin,<sup>5</sup> and Chen<sup>41</sup> have shown that silane activation on NPG can lead to the efficient oxidation of silanes to silanols, as well as transfer semi-hydrogenation of alkynes. Herein, we disclose that NPG activates Si–H bonds through a homolytic pathway, forming hydrogen radicals and [Au]–[Si] intermediates. This new activation mode allows efficient monoalcoholysis of dihydrosilanes in a controlled (only one Si–H is activated) and chemoselective (hydrogen radicals tolerate many functional groups) manner. By tuning the reaction conditions, the second Si–H bond activation/alcoholysis can proceed to give unsymmetrical silaketals in a one-pot reaction. Moreover, the [Au]–[Si] intermediates could serve as both an electrophile (forming Si–O bonds) and nucleophile (forming C–Si bonds), resulting in the ring opening/bis-silylation reaction of a range of cyclic ethers.

## Results and discussion

### Monoalcoholysis of di-*tert*-butylsilane

Our investigation started with testing a number of heterogeneous catalysts in the monoalcoholysis of di-*tert*-butylsilane (**A**) with benzyl alcohol **1a** (Table 1). Commercial Pd/C is the most reactive among the tested catalysts, however affording undesired disiloxane **3a** in a high percentage. Au–Pd alloy nanoparticles and Au nanoparticles showed moderate activity but good selectivity. These observations suggested that Au is less reactive but more selective than Pd in the monoalcoholysis. When NPG was employed, the reaction rate was significantly improved, achieving 70% conversion in 12 h (Table 1, entry 5). A synthetically useful condition was obtained at 50 °C with 92% yield of **2a** in 2 h. The turnover number (TON) and the turnover frequency (TOF) of the NPG under these conditions were

<sup>a</sup>Tsinghua-Peking Joint Centers for Life Sciences, School of Pharmaceutical Sciences, Tsinghua University, Beijing 100084, China. E-mail: whe@mail.tsinghua.edu.cn

<sup>b</sup>Tianjin Key Laboratory of Advanced Functional Porous Materials, Tianjin University of Technology, Tianjin 300384, China. E-mail: yding@tjut.edu.cn

<sup>c</sup>Department of Chemistry, Tsinghua University, Beijing 100084, China

† Electronic supplementary information (ESI) available. See DOI: 10.1039/c8sc01427b

‡ These authors contributed equally to this work.



Table 1 Monoalcoholysis of di-*tert*-butylsilane<sup>a</sup>

| Entry          | Catalyst                          | Conversion <sup>b</sup> | 2a <sup>c</sup> | 3a <sup>c</sup> |
|----------------|-----------------------------------|-------------------------|-----------------|-----------------|
| 1              | Pd/C                              | 99%                     | 60%             | 15%             |
| 2              | AuPd/C <sup>d</sup>               | 79%                     | 30%             | 11%             |
| 3              | Au/Al <sub>2</sub> O <sub>3</sub> | 25%                     | 21%             | n.d.            |
| 4              | Gold foil                         | 13%                     | 11%             | n.d.            |
| 5              | NPG                               | 70%                     | 66%             | n.d.            |
| 6 <sup>e</sup> | NPG                               | 99%                     | 92%             | n.d.            |
| 7 <sup>e</sup> | Au salt                           | 10%                     | 8%              | n.d.            |
| 8 <sup>e</sup> | —                                 | 10%                     | 8%              | n.d.            |

<sup>a</sup> Reaction conditions: **1a** (1.0 mmol), *t*-Bu<sub>2</sub>SiH<sub>2</sub> (**A**, 2.1 mmol) and catalyst (1 mol%) in toluene (5 mL) under nitrogen, 25 °C for 12 h. <sup>b</sup> Conversion monitored by NMR on the crude material. <sup>c</sup> Isolated yields. <sup>d</sup> Au–Pd alloy nanoparticles (Au 1.5%, Pd 1%, w/w) supported on activated carbon, 1 mol% based on metal. <sup>e</sup> 50 °C, 2 h. n.d. = not detected.

calculated to be as high as 5377 and 2689 h<sup>-1</sup>, respectively (Table 1, entry 6). Such a high TOF and TON highlight the activity enhancement brought by the nanostructure of the NPG. In contrast, homogeneous Au salts,<sup>8</sup> such as 0.5 ppm AuCl or AuCl<sub>3</sub> solutions showed a very low conversion even at 50 °C (Table 1, entry 7), which is similar to the control reaction without any catalyst (Table 1, entry 8), suggesting that the homogenous Au salts did not contribute to the reaction.

### EPR study

With great curiosity we sought to understand the intrinsic selectivity of NPG by probing how the NPG catalyst activates the dihydrosilanes. To this end, we employed the electron paramagnetic resonance (EPR) spectroscopy using PBN as the spin trap (Fig. 1).<sup>42</sup> Under our model reaction conditions, a persistent signal attributed to the PBN-H adduct was observed (Fig. 1a, *a*<sub>N</sub> = 15.26 G, *a*<sub>H(1)}</sub> = *a*<sub>H(2)}</sub> = 7.60 G).<sup>42,43</sup> A similar radical was observed in the absence of the benzyl alcohol under otherwise identical conditions (Fig. 1b, *a*<sub>N</sub> = 15.00 G, *a*<sub>H(1)}</sub> = *a*<sub>H(2)}</sub> = 7.28 G). However, no signal was detected in the absence of the di-*tert*-butylsilane (Fig. 1c and d). Collectively, these results suggested that the radical originated from the di-*tert*-butylsilane but not the benzyl alcohol<sup>44</sup> nor the solvent toluene. Interestingly, EPR of the silane alone in the toluene also gave weak radical signals (Fig. 1e), which is consistent with the spontaneous reaction without a catalyst (Table 1, entry 8). In contrast, the trapping of a silyl radical<sup>44</sup> by PBN was not observed, suggesting the silyl moiety is still covalently linked to the gold surface ([Au]–[Si] species). Such a homolytic Si–H activation by the NPG is consistent with the earlier observations of Raffa,<sup>39</sup> and is completely different from that by the homogeneous gold catalysts. In the latter cases, discrete [Au]–H was responsible for the catalytic activity and no [Au]–[Si] intermediate was ever proposed.<sup>45,46</sup>

Similar behaviour was also observed with the less hindered, more reactive diethylsilane (Fig. 1f, *a*<sub>N</sub> = 14.43 G, *a*<sub>H</sub> = 7.54 G).

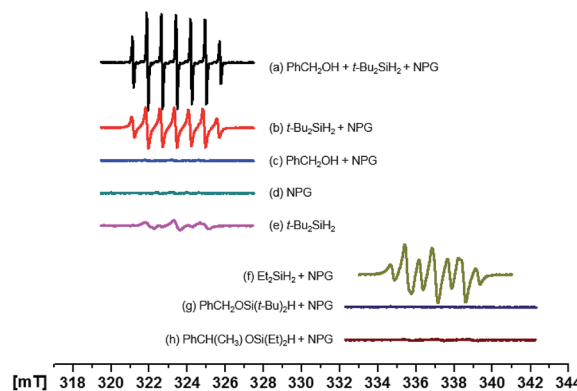
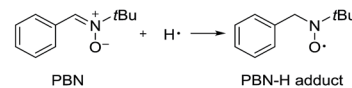


Fig. 1 EPR spectra using PBN (0.02 mmol) as the spin trap. In respective tests, 0.5 mL toluene solvent was used. Other reagents if used: alcohol (0.15 mmol), silane (0.23 mmol), and NPG (0.015 mmol). Tests (a–e) were run at 0 °C after reaction at 50 °C for 5 min. Tests (f–h) were run at r.t. after reaction at r.t. for 10 min.

However, when two representative hydrosilyl ethers **2a** (Fig. 1g) and **2r** (Fig. 1h) were submitted to the EPR experiments, no PBN-H adduct was observed. These data suggested that the activation of the Si–H bonds in the hydrosilyl ethers by the NPG was much slower. The steric and electronic differences brought by the alkoxy substitutions might account for the retarded Si–H activation on the NPG surface. Altogether, it is clear that the selective activation of the first Si–H bond in dihydrosilane by NPG is the origin of the observed monoalcoholysis.

### Scope of the NPG catalysed monoalcoholysis

Based on the observed selective homolytic Si–H activation of dihydrosilanes with NPG, we demonstrated the scope of the monoalcoholysis (Table 2). Primary (**1a–1c**, **1j–1o**) and secondary (**1d–1f**) alcohols are shown to be compatible with the current method, affording the desired hydrosilyl ethers. Reactions of tertiary alcohols (**1g**, **1h**) with di-*tert*-butylsilane were slow. However, using diethylsilane instead led to excellent isolated yields of the desired products (**2g** and **2h**). Phenol was also successfully converted into silane **2i**, a precursor for *ortho*-C–H alkenylation.<sup>47</sup> Mono silylation of substrates bearing two hydroxyl groups could also be achieved by controlling the stoichiometry of the dihydrosilane. In the presence of 1.0 equiv. of the di-*tert*-butylsilane, mono silylation of  $\alpha,\omega$ -diol gave a high yield of the desired product (**2m**), which might suggest that the absorption of **1m** onto the surface of the NPG is faster than that of **2m**. Moreover, the primary hydroxyl was selectively silylated over the secondary hydroxyl (**2n**), and the benzyl alcohol was selectively silylated over the phenol (**2o**). The two cases indicate that the primary alcohols are more reactive than secondary alcohols and phenols under the current reaction conditions.

The current method showed excellent compatibility with a range of reducible functionalities, since the hydrogen radicals are much less reactive than the metal hydride. The internal





Table 3 Ring-opening/silylation of cyclic ethers<sup>a</sup>

| Entry          | Cyclic ether <b>7</b> | Condition      | Products, yields |
|----------------|-----------------------|----------------|------------------|
| 1              |                       | 0–50 °C, 0.5 h | <br>             |
| 2 <sup>b</sup> |                       | 50 °C, 3 h     | <br>             |
| 3              |                       | 90 °C, 7 h     | <br>             |
| 4              |                       | 90 °C, 36 h    | n.d.<br>         |

<sup>a</sup> Products and isolated yields of the NPG catalysed ring opening silylation reaction. Conditions: unless otherwise specified, cyclic ether (3.0 mmol), *t*-Bu<sub>2</sub>SiH<sub>2</sub> (6.6 mmol) and catalyst (3 mol%), under argon, in a sealed tube. <sup>b</sup> Toluene 1 mL was added as the solvent. n. d. = not detected.

Si and a C–Si bond. In hindsight, the direct hydrosilylation of cyclic ethers<sup>57–60</sup> had been reported in four papers, catalysed by a homogeneous iridium complex,<sup>57</sup> dicobalt octacarbonyl,<sup>58</sup> or boron Lewis acid.<sup>59,60</sup> Stratakis and co-workers reported an elegant gold nanoparticle catalysed silaboration of oxetanes and unactivated epoxides. This interesting formal addition of Si–B was proposed to proceed through the oxidative insertion of Au into Si–B bonds, which is different than our radical pathway (*vide infra*).<sup>61</sup> Others examples were limited to the ring-opening bromo- or iodo-silylation with Br- or I-silanes<sup>62</sup> or its synthetic equivalents.<sup>63</sup> Notably, our NPG catalysis provides a different bis-functionalization method, affording bis-silicons that could serve as useful building blocks in organic syntheses and materials chemistry. For example, the chemoselective O–Si cleavage of the bis-silicon **9c** was successfully achieved under TBAF conditions, affording a terminal alcohol synthon (see ESI 5.1†). The versatile reactivity of the remaining silane bond also provides ample synthetic opportunities, including the preparation of silicone monomers.

To further probe the reaction scope as well as to shed light on the mechanism of the reaction, substituted cyclic ethers were then studied (Table 4). Overall, the reactivity of the substituted cyclic ethers (mainly hydrosilylation) is very different than that of the unsubstituted ones (mainly bis-silylation). Three conspicuous trends could be summarized from the data: (1) the incorporation of a substituent on the carbon next to the

Table 4 Ring-opening/silylation of substituted cyclic ethers<sup>a</sup>

| Entry          | <b>7</b> | Products, yields |
|----------------|----------|------------------|
| 1              |          | <br>             |
| 2              |          | <br>             |
| 3              |          | <br><br>         |
| 4 <sup>b</sup> |          | <br>             |
| 5 <sup>c</sup> |          |                  |
| 6 <sup>c</sup> |          | <br>             |
| 7 <sup>c</sup> |          | <br>             |
| 8 <sup>d</sup> |          |                  |

<sup>a</sup> Products and isolated yields of the NPG catalysed ring-opening silylation reaction. Conditions: unless otherwise specified, cyclic ether (3.0 mmol), *t*-Bu<sub>2</sub>SiH<sub>2</sub> (6.6 mmol) and catalyst (3 mol%), under argon, in a sealed tube, 40 °C, 4 h. <sup>b</sup> Toluene 2 mL as the solvent, 70 °C, 5 h. <sup>c</sup> 70 °C, 5 h. <sup>d</sup> 90 °C, 15 h.

oxygen atom shut down the bis-silylation (**7e–7l**), while a substituent further away resulted in bis-silylation (*cf.* **7l** and **7m**). The hydrosilylation of **7g**, **7h**, **7i** and **7l** is not what we intended, but the yields are high. The bis-silylation of **7m** and **7n** is very efficient. (2) The ring opening took place preferentially at the more substituted carbon (*cf.* **7e**, **7f**, and **7l**), with the only exception in the case of **7n** (*vide infra*); (3) when a quaternary carbon (**7k**) or a carbon connected with phenyl groups (**7f**, **7j** and **7l**) is present in the substrate, elimination products were observed. The elimination products (*i.e.*, **10**) alerted us to a possible elimination–hydrosilylation pathway. To this end, an independently synthesized (but-3-enyloxy)di-*tert*-butylsilane



failed to produce the desired product **9c** under the reaction conditions (see ESI†), which was consistent with the chemoselectivity shown in Table 2 (*cf.* **2p**) and suggested that the C–Si bond formation is unlikely to proceed through an elimination–hydrosilylation sequence.

A plausible mechanism of this cyclic ether ring opening/bis-silylation reaction is proposed (Fig. 3), which could explain our experimental observations. First, the Si–H bond of silane is activated on the surface of NPG, possibly in an oxidative-insertion manner, which gave the intermediate **A**. The Au–H bond is more susceptible to the PBN trapping than the Au–Si bond, so that only the hydrogen radical was observed. We observed hydrogen gas formation in the reaction, which is associated with the formation of species **B** from species **A**. The formations of hydrogen gas and Au–Si species of type **A** were also documented by the Stratakis group in their Au/TiO<sub>2</sub> NP catalysed *cis*-1,2-disilylation of alkynes.<sup>64</sup> We believe that at higher temperature the formation of hydrogen gas was more favourable, thus the ratio of **B/A** becomes bigger. A radical type C–O bond cleavage of the cyclic ether can be triggered either by the intermediate **A** or by the intermediate **B**, leaving the radical on the more substituted carbon (*i.e.*, **C**). We proposed this radical was instantly trapped by the NPG surface, thus forming the intermediate **D**. The fate of the intermediate **D** diverges depending on the substrate structure. When it is a highly stable benzyl radical, it undergoes elimination to give alkene products (*e.g.* **10f**). It also could form the hydrosilylation products by a formal hydrogen shift on the surface of **A**, or form the bis-silylation product through a formal Si shift on the surface of **B**. The higher population of **B** at higher temperature explains the higher yields of bis-silylation products. This mechanism can also explain why most of the substituted cyclic ethers underwent hydrosilylation but not bis-silylation. The reason might lie in the steric difference. When there is a R group attached to the carbon linked to the Au surface, the Si shift is considerably more sterically demanding than the H shift. In the case of **7n**, the successful formation of the bis-silylation product **9n** is the result of both a higher reaction temperature and less steric repulsion. It should be noted that with a larger ring system, the organic compound depicted in intermediate **D** would have more flexibility to avoid repulsion with the Au surface, therefore rendering it possible to cleave the C–O bond in an opposite

position. Such a mechanistic proposal is intriguing in two aspects: (1) the reaction selectivity is very much dependent on the surface reactivity of the catalyst; (2) the [Au]–[Si] species formally serves as both an electrophile and a nucleophile in this bis-silylation ring-opening reaction. Both aspects cannot be achieved by homogeneous catalysis.

## Conclusions

In conclusion, by virtue of the NPG catalysed homolytic NPG activation of Si–H bonds, we realized three new silylation reactions: controlled monoalcoholysis of dihydrosilanes, one-pot formation of unsymmetrical silaketals and ring-opening bis-silylation of cyclic ethers. These reactions feature a readily available catalyst, operationally simple protocols and high efficiencies. Moreover, the high chemoselectivity and functional group compatibility achieved by this NPG catalysis are unprecedented in the literature. Together with the exotic amphiphilic reactivity of [Au]–[Si] intermediates, this study showcased the unique potential of heterogeneous catalysts in organic syntheses.

## Conflicts of interest

There are no conflicts to declare.

## Acknowledgements

This work is supported by the National Key R&D Program of China (No. 2017YFA0505200) and NSFC (21625104 and 21521091).

## References

- 1 B. Marciniec, *Hydrosilylation: a comprehensive review on recent advances*, Springer Science & Business Media, 2008.
- 2 S. E. Denmark and M. H. Ober, *Aldrichimica Acta*, 2003, **36**, 75–85.
- 3 C. Cheng and J. F. Hartwig, *Chem. Rev.*, 2015, **115**, 8946–8975.
- 4 S. Bähr and M. Oestreich, *Angew. Chem., Int. Ed.*, 2017, **56**, 52–59.
- 5 M. Yan, T. Jin, Y. Ishikawa, T. Minato, T. Fujita, L. Y. Chen, M. Bao, N. Asao, M. W. Chen and Y. Yamamoto, *J. Am. Chem. Soc.*, 2012, **134**, 17536–17542.
- 6 M. Yan, T. A. Jin, Q. Chen, H. E. Ho, T. Fujita, L. Y. Chen, M. Bao, M. W. Chen, N. Asao and Y. Yamamoto, *Org. Lett.*, 2013, **15**, 1484–1487.
- 7 L. Zamostna, M. Ahrens and T. Braun, *J. Fluorine Chem.*, 2013, **155**, 132–142.
- 8 H. F. Guo, X. L. Yan, Y. Zhi, Z. W. Li, C. Wu, C. L. Zhao, J. Wang, Z. X. Yu, Y. Ding, W. He and Y. D. Li, *Nano Res.*, 2015, **8**, 1365–1372.
- 9 Y. Sumida, T. Kato, S. Yoshida and T. Hosoya, *Org. Lett.*, 2012, **14**, 1552–1555.
- 10 T. A. Boebel and J. F. Hartwig, *J. Am. Chem. Soc.*, 2008, **130**, 7534–7535.

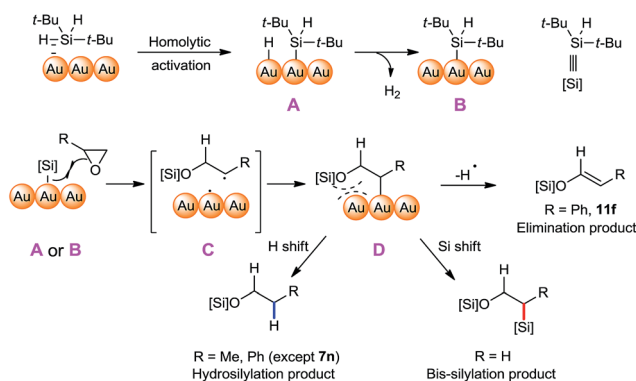


Fig. 3 Proposed mechanism of the ring-opening reaction.



- 11 E. M. Simmons and J. F. Hartwig, *J. Am. Chem. Soc.*, 2010, **132**, 17092–17095.
- 12 E. M. Simmons and J. F. Hartwig, *Nature*, 2012, **483**, 70–73.
- 13 D. Sieh and P. Burger, *J. Am. Chem. Soc.*, 2013, **135**, 3971–3982.
- 14 J. A. Muchnij, F. B. Kwaramba and R. J. Rahaim, *Org. Lett.*, 2014, **16**, 1330–1333.
- 15 Y. Hua, P. Asgari, T. Avullala and J. Jeon, *J. Am. Chem. Soc.*, 2016, **138**, 7982–7991.
- 16 S. J. O'Malley and J. L. Leighton, *Angew. Chem., Int. Ed.*, 2001, **40**, 2915–2917.
- 17 J. T. Spletstoser, M. J. Zacuto and J. L. Leighton, *Org. Lett.*, 2008, **10**, 5593–5596.
- 18 T. Lee and J. F. Hartwig, *Angew. Chem., Int. Ed.*, 2016, **55**, 8723–8727.
- 19 T. Zell, T. Schaub, K. Radacki and U. Radius, *Dalton Trans.*, 2011, **40**, 1852–1854.
- 20 I. Buslov, J. Becouse, S. Mazza, M. Montandonclerc and X. Hu, *Angew. Chem., Int. Ed.*, 2015, **54**, 14523.
- 21 F. Kakiuchi, K. Tsuchiya, M. Matsumoto, B. Mizushima and N. Chatani, *J. Am. Chem. Soc.*, 2004, **126**, 12792–12793.
- 22 S. T. Ding, L. J. Song, Y. Wang, X. H. Zhang, L. W. Chung, Y. D. Wu and J. W. Sun, *Angew. Chem., Int. Ed.*, 2015, **54**, 5632–5635.
- 23 S. Wübbolt and M. Oestreich, *Angew. Chem., Int. Ed.*, 2015, **54**, 15876–15879.
- 24 W. Li, X. Huang and J. You, *Org. Lett.*, 2016, **47**, 666–668.
- 25 C. Chen, M. B. Hecht, A. Kavara, W. W. Brennessel, B. Q. Mercado, D. J. Weix and P. L. Holland, *J. Am. Chem. Soc.*, 2015, **137**, 13244–13247.
- 26 H. Nishiyama and A. Furuta, *Chem. Commun.*, 2007, **7**, 760–762.
- 27 J. Y. Wu, B. N. Stanzl and T. Ritter, *J. Am. Chem. Soc.*, 2010, **132**, 13214–13216.
- 28 D. J. Peng, Y. L. Zhang, X. Y. Du, L. Zhang, X. B. Leng, M. D. Walter and Z. Huang, *J. Am. Chem. Soc.*, 2013, **135**, 19154–19166.
- 29 J. H. Chen, B. Cheng, M. Y. Cao and Z. Lu, *Angew. Chem., Int. Ed.*, 2015, **54**, 4661–4664.
- 30 Z. Q. Zuo, L. Zhang, X. B. Leng and Z. Huang, *Chem. Commun.*, 2015, **51**, 5073–5076.
- 31 M. Moreno-Manas and R. Pleixats, *Acc. Chem. Res.*, 2003, **36**, 638–643.
- 32 M. Pagliaro, V. Pandarus, R. Ciriminna, F. Beland and P. D. Cara, *ChemCatChem*, 2012, **4**, 432–445.
- 33 F. Zaera, *Chem. Soc. Rev.*, 2013, **42**, 2746–2762.
- 34 H. A. Cong, C. F. Becker, S. J. Elliott, M. W. Grinstaff and J. A. Porco, *J. Am. Chem. Soc.*, 2010, **132**, 7514–7518.
- 35 D. T. D. Tang, K. D. Collins and F. Glorius, *J. Am. Chem. Soc.*, 2013, **135**, 7450–7453.
- 36 B. Xiao, Z. Q. Niu, Y. G. Wang, W. Jia, J. Shang, L. Zhang, D. S. Wang, Y. Fu, J. Zeng, W. He, K. Wu, J. Li, J. L. Yang, L. Liu and Y. D. Li, *J. Am. Chem. Soc.*, 2015, **137**, 3791–3794.
- 37 Y. Zhang, X. Cui, F. Shi and Y. Deng, *Chem. Rev.*, 2012, **112**, 2467–2505.
- 38 M. Stratakis and H. Garcia, *Chem. Rev.*, 2012, **112**, 4469–4506.
- 39 P. Raffa, C. Evangelisti, G. Vitulli and P. Salvadori, *Tetrahedron Lett.*, 2008, **49**, 3221–3224.
- 40 N. Asao, Y. Ishikawa, N. Hatakeyama, Menggenbateer, Y. Yamamoto, M. W. Chen, W. Zhang and A. Inoue, *Angew. Chem., Int. Ed.*, 2010, **49**, 10093–10095.
- 41 T. Fujita, P. F. Guan, K. McKenna, X. Y. Lang, A. Hirata, L. Zhang, T. Tokunaga, S. Arai, Y. Yamamoto, N. Tanaka, Y. Ishikawa, N. Asao, Y. Yamamoto, J. Erlebacher and M. W. Chen, *Nat. Mater.*, 2012, **11**, 775–780.
- 42 M. Conte, H. Miyamura, S. Kobayashi and V. Chechik, *J. Am. Chem. Soc.*, 2009, **131**, 7189–7196.
- 43 E. G. Janzen, T. Kasai and K. Kuwata, *Bull. Chem. Soc. Jpn.*, 1973, **46**, 2061–2062.
- 44 J. Zeitouny and V. Jouikov, *Phys. Chem. Chem. Phys.*, 2009, **11**, 7161–7170.
- 45 H. Ito, T. Saito, T. Miyahara, C. M. Zhong and M. Sawamura, *Organometallics*, 2009, **28**, 4829–4840.
- 46 S. Labouille, A. Escalle-Lewis, Y. Jean, N. Mezailles and P. Le Floch, *Chem.–Eur. J.*, 2011, **17**, 2256–2265.
- 47 M. Mewald, J. A. Schiffner and M. Oestreich, *Angew. Chem., Int. Ed.*, 2012, **51**, 1763–1765.
- 48 A. M. Caporusso, L. A. Aronica, E. Schiavi, G. Martra, G. Vitulli and P. Salvadori, *J. Organomet. Chem.*, 2005, **690**, 1063–1066.
- 49 A. Corma, C. Gonzalez-Arellano, M. Iglesias and F. Sanchez, *Angew. Chem., Int. Ed.*, 2007, **46**, 7820–7822.
- 50 J. Ohshita, R. Taketsugu, Y. Nakahara and A. Kunai, *J. Organomet. Chem.*, 2004, **689**, 3258–3264.
- 51 R. J. P. Corriu and J. J. E. Moreau, *J. Chem. Soc., Chem. Commun.*, 1973, 38–39.
- 52 D. Mukherjee, R. R. Thompson, A. Ellern and A. D. Sadow, *ACS Catal.*, 2011, **1**, 698–702.
- 53 C. Lorenz and U. S. Schubert, *Chem. Ber.*, 1995, **128**, 1267–1269.
- 54 S. Bracegirdle and E. A. Anderson, *Chem. Soc. Rev.*, 2010, **39**, 4114–4129.
- 55 C. N. Scott and C. S. Wilcox, *Synthesis*, 2004, **36**, 2273–2276.
- 56 C. N. Scott and C. S. Wilcox, *J. Org. Chem.*, 2010, **75**, 253–256.
- 57 S. Park and M. Brookhart, *Chem. Commun.*, 2011, **47**, 3643–3645.
- 58 K. T. Kang and W. P. Weber, *Tetrahedron Lett.*, 1985, **26**, 5753–5754.
- 59 J. B. Grande, D. B. Thompson, F. Gonzaga and M. A. Brook, *Chem. Commun.*, 2010, **46**, 4988–4990.
- 60 M. Gevorgyan, S. Rubin, J. Benson, J.-X. Liu and Y. Yamamoto, *J. Org. Chem.*, 2000, **65**, 6179–6186.
- 61 E. Vasilikogiannaki, A. Louka and M. Stratakis, *Organometallics*, 2016, **35**, 3895–3902.
- 62 U. Kruerke, *Chem. Ber.*, 1962, **95**, 174–182.
- 63 J. Ohshita, A. Iwata, F. Kanetani, A. Kunai, Y. Yamamoto and C. Matui, *J. Org. Chem.*, 1999, **64**, 8024–8026.
- 64 I. Saridakis, M. Kidonakis and M. Stratakis, *ChemCatChem*, 2018, **10**, 980–983.

